

Monte Carlo Simulation of Electron Beams produced by LIAC Intraoperative Radiation Therapy Accelerator

Robotjazi M.¹, Tanha K.², Mahdavi S. R.^{3*}, Baghani H. R.⁴, Mirzaei H. R.⁵, Mousavi M.¹, Nafissi N.⁶, Akbari E.⁷

ABSTRACT

Background: One of the main problems of dedicated IORT accelerators is to determine dosimetric characteristics of the electron beams. Monte Carlo simulation of IORT accelerator head and produced beam will be useful to improve the accuracy of beam dosimetry.

Materials and Methods: Liac accelerator head was modeled using the BEAM-nrcMonte Carlo simulation system. Phase-space files were generated at the bottom of the applicators. These phase-space files were used as an input source in DOSXYZnrc and BEAMDP codes for dose calculation and analysis of the characteristic of the electron beams in all applicators and energies.

Results: The results of Monte Carlo calculations are in very close agreement with the measurements. There is a decrease in the peak of the initial spectrum when electrons come from the end of accelerator wave guide to the end of applicator. By decreasing the applicator diameter, the mean energy of electron beam decreased. Using applicators and increasing their size, X-ray contamination will increase. The percentage of X-ray contamination increases by applicator diameter. This is related to the increase of the mean energy of electron beams.

Conclusion: Application of PMMA collimator leads to, although well below accepted level, the production of bremsstrahlung. The results of this study showed that special design of LIAC head accompanying by PMMA collimator system cause to produce an electron beam with an individual dosimetric characteristic making it a useful tool for intraoperative radiotherapy purposes.

Keywords

Monte Carlo Simulation, IORT, Photon Contamination, Dosimetry, LIAC

Introduction

Intraoperative radiation therapy (IORT) refers to the delivery of a single high dose of irradiation directly to the tumor bed after removal of the tumor. Besides the advantage of direct access to the irradiation site, IORT may also permit to preserve healthy neighboring organs either by dislodging them from the bulk of the radiation field or by interposing shielding between them and the target area.

One of the main problems of dedicated IORT accelerators is to determine dosimetric characteristics of the electron beams that is considerably different from those obtained with conventional accelerators, due to different design of the head and the collimation system [1]. In addition,

¹Medical Physics and Radiological Sciences Department, Sabzevar University of Medical Sciences, Sabzevar, Iran

²Persian Gulf Nuclear Medicine Research Center, Bushehr University of Medical Sciences, Bushehr, Iran

³Medical Physics Department, Iran University of Medical Sciences, Tehran, Iran

⁴Physics Department, School of Sciences, Hakim Sabzevari University, Sabzevar, Iran

⁵Radiation Therapy Department, Shahid Beheshti University of Medical Sciences, Tehran, Iran

⁶Surgery Department, Iran University of Medical Sciences, Tehran, Iran

⁷Oncological Surgery Department, Shahid Beheshti University of Medical Sciences, Tehran, Iran

*Corresponding author: S. R. Mahdavi, Medical Physics Department, Iran University of Medical Sciences, Tehran, Iran
E-mail: srmahdavi@hotmail.com

Received: 16 February 2016
Accepted: 8 July 2016

these accelerators have a very high dose per pulse electron beam which strongly reduces the irradiation time to achieve the prescribed dose. In other words, calibration of electron beam produced by such accelerators using ion chambers is not a simple task. The presence of high dose per pulse electron beam causes some degrees of uncertainty in absolute and relative dosimetries [2, 3]. Monte Carlo simulation of IORT accelerator head and produced beam will be useful to improve the accuracy of beam dosimetry and will reduce the number of dosimetric measurements. Some studies investigated the dosimetric parameters of electron beams generated by dedicated IORT accelerators [4, 5]. However, some dosimetric parameters and their effects on dose distribution have not been considered in these studies.

In this work, we benchmarked the Monte Carlo simulation of IORT electron beam by comparing measured and calculated dose distributions in water. The main aim of this work was to analyze some missed dosimetric parameters of LIAC IORT accelerator using Monte Carlo simulation which have not been stated in previous studies.

Material and Methods

Liac® IORT Accelerator

The Liac® system (Spa, Sordina, Italy) is a dedicated mobile linac of IORT. Two Liac®

models with two nominal energy ranges (4, 6, 8, 10 MeV and 6, 8, 10, 12 MeV) are available. The 12 MeV model which has been used in this work, contains a vacuum exit window (titanium) and an aluminum scattering foil. The Liac equipped with 5mm thickness and 600mm long polymethyl methacrylate (PMMA) cylindrical applicators with diameter between 3cm to 10cm. Furthermore, the applicators are available in beveled forms at angles of 15, 30 and 45 degrees. Source-to-Surface Distance (SSD) of this linac is 71.3 cm [5].

Monte Carlo Simulation

The Liac® accelerator head was modeled using BEAMnrc Monte Carlo simulation system [6, 7]. The geometry of Liac® head includes the exit window, scattering foil, monitor ion chamber and different applicators provided by the manufacturer and modeled using BEAMnrc component modules (CM) (Table 1, Figure 1).

The electron beam source was modeled by ISOURC=19 module which is circular beam with 2D Gaussian distribution. To drive the best estimation of full width of half maximum (FWHM) of the electron beam, four different simulations were performed for 1mm, 2mm, 3mm and 4mm FWHMs of the electron beam. As there were no significant differences among results, the FWHM was set to 2mm.

Table 1: The list of component modules and their materials for Liac machine are tabulated

Liac® component	CM	Material
Titanium window	SLAB	Titanium (TI)
Scattering foil	SLAB	Aluminum (AL)
Monitor unit chamber	CHAMBER	Aluminum (AL), Air (AIR) and Mylar (MYLAR)
Applicator	FLATFILT	PMMA
Surrounding structures	FLATFILT	Steel (STEEL) for base of titanium Peek* (PEEK) for up

* The material PEEK was added to PEG4 for construction the inner section of the accelerator.

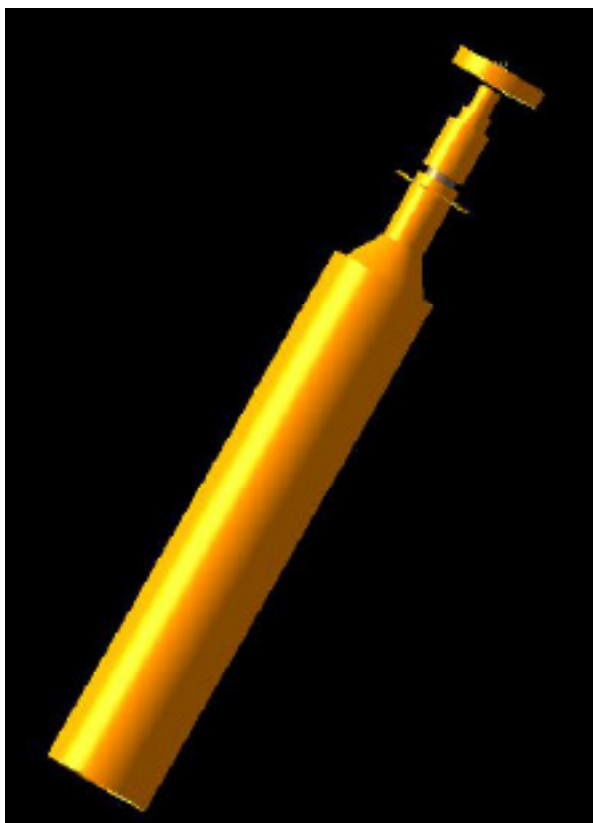


Figure 1: 3D images of LIAC head and reference applicator simulation obtained from EGS-Window user codes

Transport parameters included ECUT and PCUT which are used to define the global electron and photon cut-off energies, were set to 0.521 MeV and 0.01 MeV, respectively. No variance reduction techniques were used. To assure statistical accuracy, the number of histories was selected as 3×10^8 for each simulation. Default values were used for the parameters reduced electron step transport algorithm (PRESTA-II) in all simulations [8].

Phase-space files which contain information about the energy, charge, position and direction of each particle, were generated at the bottom of the applicators. Then, these phase-space files were used as an input source at the surface of the phantom for dose calculation in water phantom using DOSXYZnrc code [9]. The dimensions and the voxel size of water phantom were set to $30 \times 30 \times 15 \text{ cm}^3$ and $2 \times 2 \times 2 \text{ mm}^3$, respectively. For the purpose of Monte Carlo

tuning, calculated and measured PDD and TDP of reference applicator were considered to be matched. For better comparison between Monte Carlo calculations and measurements, each TDP and PDD curves were normalized to the center of the curve and depth of maximum dose, respectively. To evaluate the agreement of PDDs and TDPs between MC simulation and experimental values, gamma analysis was used proposed by Low et al. [10]. Gamma analysis is a comparison tool that simultaneously combines dose difference (DD) and distance-to-agreement (DTA) criterion. DD and DTA criteria in calculations of gamma index were set as 2% and 2 mm, respectively [11]. Gamma index values between zero to one were considered as a passed (agreement between obtained results), while values greater than one were considered as a failed (disagreement between the obtained results). It should be mentioned that the gamma index calculations were performed by Dose Lab Pro (Mobius Medical Systems, LP, Houston, TX).

After tuning of Monte Carlo, all applicators for all nominal energies of LIAC were simulated in BEAMnrc code. The PDD and TDP for all energies and applicators were calculated using DOSXYZnrc code.

The phase-space files of different energies at the end of applicators were used as an input file for BEAMDP code to analyse the characteristic of the electron beams. We used BEAMDP code to obtain the electron energy spectra, electron frounce, the mean and probable energy distributions of the electrons at the phantom surface for all applicator and energies, as well as the angular distributions of the electrons at the phantom surface.

Experimental Measurements

For comparison of Monte Carlo calculations with absorbed dose measurements, dose profiles were obtained using a calibrated Advanced Markus ion chamber (PTW, Freiburg) and a MP3 water phantom (PTW, Freiburg) at the depth of maximum dose (D_{max}). Also,

PDDs were measured along the central axes of different beams to validate the simulations.

Results

Figure 2 shows measured and calculated PDD along the beam axis using reference applicator for all nominal energies.

Figure 3 shows the variation of PDD curves of different electron beams at various applicator sizes. As mentioned, LIAC accelerator uses the cylindrical applicator for electron beam collimation. This kind of beam collimation causes a greater decrease in the average of beam energy at the end of the applicator due to the multiple scattering of electrons from applicator wall. Quantitative analysis was conducted for the variations of beam energy using these applicators and effect of changing energy on PDD curves by PTW MEPHYSTO beam analysing software. X-ray contamina-

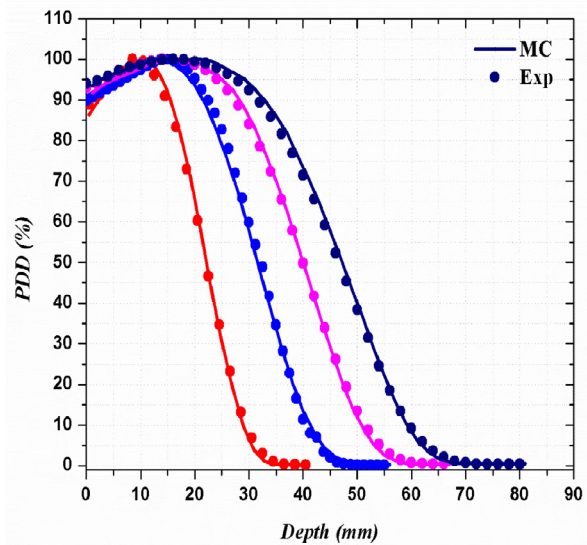


Figure 2: Measured (Advanced-Markus) and calculated (Monte Carlo) PDDs in water along the central beam axis. The 6, 8, 10, 12 MeV PDDs are shown in Red, Blue, Pink, and Navy colors, respectively.

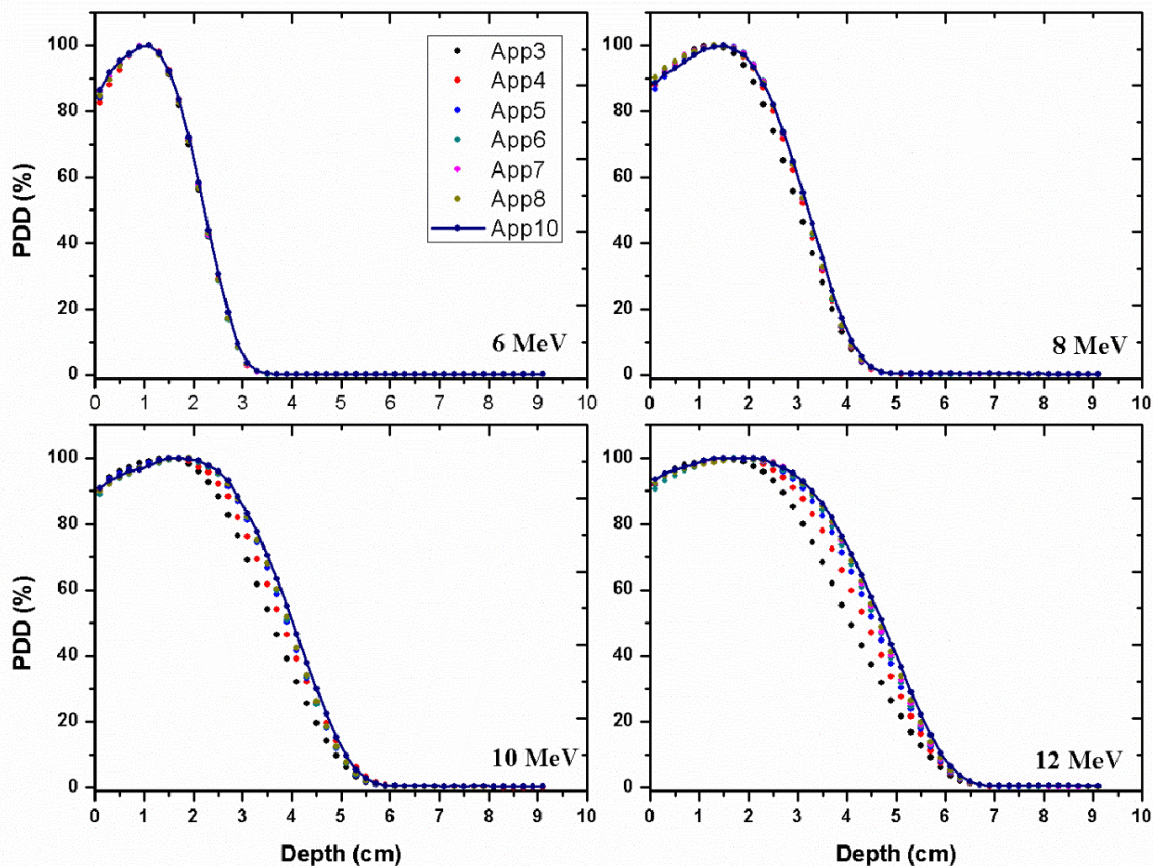


Figure 3: PDD curves of different electron beams at various applicator sizes.

tion, probable and mean energy for all energy and applicator ranges were extracted from this software and are shown in Table 2.

Figure 4 represents the calculated and measured dose profiles of all nominal energies of LIAC for reference applicator at D_{max} . There was a good agreement between calculated and experimental dose profiles for all nominal energies and applicators.

Dose profiles are also shown at D_{max} for all applicators with nominal electron energy of 12 MeV in Figure 5.

Figure 6 shows the energy spectra for the nominal energies of 6, 8, 10 and 12 MeV for the reference field size obtained from BEAM-DP at the phantom surface against the primary electron spectra at the level of the titanium window provided by the manufacturer [12]. Moreover, the electron energy spectra for 12 MeV beam using applicators with 3, 4, 5, 6, 7, 8 and 10 cm diameters are shown in Figure 7.

The electron and photon fluence profiles of all nominal energies at the exit of reference applicator are shown in Figure 8. For the purpose of illustration of PMMA collimator effect in the bremsstrahlung production, photon and electron fluence profiles are shown separately.

Discussion

In the present work, experimental measurements have been used to benchmark the Monte Carlo simulation of IORT electron beam to evaluate the beam characteristics such as the energy spectra and the fluence of the electron and photon beam for all nominal energies degraded from dedicated IORT linac.

In order to verify and ensure the accuracy of the accelerator's head modelling, Monte Carlo calculations were compared to experimental measurements in the water phantom for all energies and applicator sizes in terms of PDD and TDP. It can be seen that the results of Monte Carlo calculations are in very close agreement with the measurements. The gamma values for PDD and dose profiles were passed in >95% of cases.

As it can be seen in Figure 1, using electron beam energy spectrum on the top of the titanium window, there is no significant disagreement between Monte Carlo and measurement in the build-up region. This is while as reported in the literature [5, 13, 14], using the mono-energetic initial electron beams in the simulations is not sufficient for a good agreement and will cause the underestimation of the simulated PDD curves in the build-up region.

Table 2: X-ray contamination, probable energy and mean energy in all energies and applicators

	6 Mev			8 Mev			10 Mev			12 Mev		
	X-ray (%)	Mean E (MeV)	Probable E (MeV)	X-ray (%)	Mean E (MeV)	Probable E (MeV)	X-ray (%)	Mean E (MeV)	Probable E (MeV)	X-ray (%)	Mean E (MeV)	Probable E (MeV)
Open	0.08	5.30	5.92	0.33	7.8	8.66	0.44	9.78	10.78	0.56	11.42	12.37
3	0.14	5.10	5.97	0.22	7.04	8.34	0.30	8.40	10.03	0.49	9.50	11.58
4	0.16	5.14	5.96	0.26	7.31	8.39	0.30	8.87	10.43	0.44	10.26	12.04
5	0.18	5.14	5.93	0.29	7.37	8.37	0.38	9.10	10.34	0.47	10.60	12.11
6	0.20	5.12	5.94	0.32	7.37	8.38	0.42	9.14	10.30	0.53	10.74	12.13
7	0.22	5.13	5.94	0.34	7.37	8.43	0.45	9.17	10.29	0.57	10.78	12.17
8	0.22	5.12	6.02	0.37	7.39	8.42	0.45	9.17	10.29	0.59	10.86	12.25
10	0.23	5.16	6.02	0.39	7.48	8.63	0.52	9.36	10.54	0.62	11.01	12.44

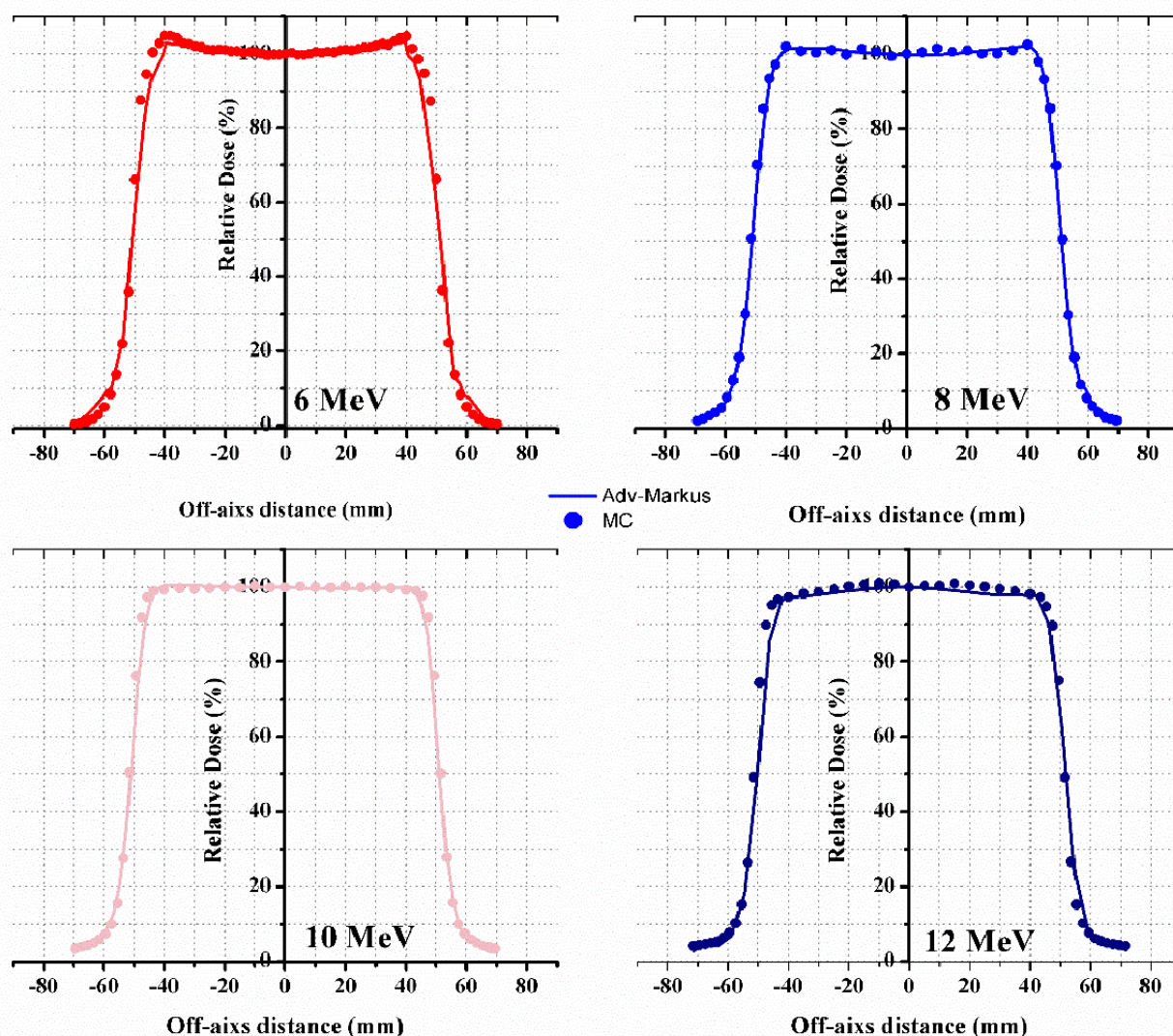


Figure 4: Measured (Advanced-Markus) and calculated (Monte Carlo) Dose profiles in water for all of the nominal beam energies of LIAC at the D_{max} .

The main cause of contribution of these low energy components in the initial spectrum of electron source is due to the absence of the bending magnet in LIAC structure. So, these low energy components cannot be removed from output electron beam at the exit of IORT applicator.

As the modelling of the accelerator head plays an important role in the shape of the dose profiles, calculated dose profiles at D_{max} in the water phantom were compared with measurements in order to evaluate the accuracy of Monte Carlo modelling. As it can be seen in Figures 2 and 3, there is a good agree-

ment between Monte Carlo calculation and measurement curves in both dose plateau and the penumbra regions. For all applicators and energies, results of the calculations are under the acceptance limits (%2 and 2mm for DD and DTA, respectively).

One of the important issues in tuning of Monte Carlo simulation is accuracy of the TDPs of electron beams in water phantom. The known-effective parameters in the accuracy of TDPs are mean angular spread and FWHM of selected source on top of the titanium window. In agreement with previous studies, our calculated TDPs using Monte Carlo did not change

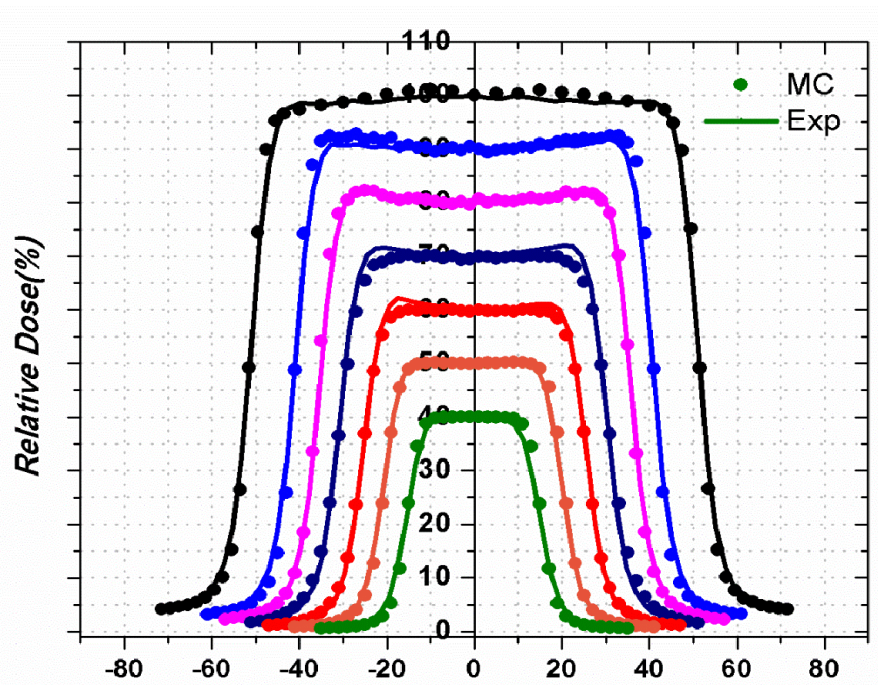


Figure 5: Measured (Advanced-Markus) and calculated (Monte Carlo) dose profiles for applicators with diameters of 3 to 10 cm with nominal energy of 12 MeV.

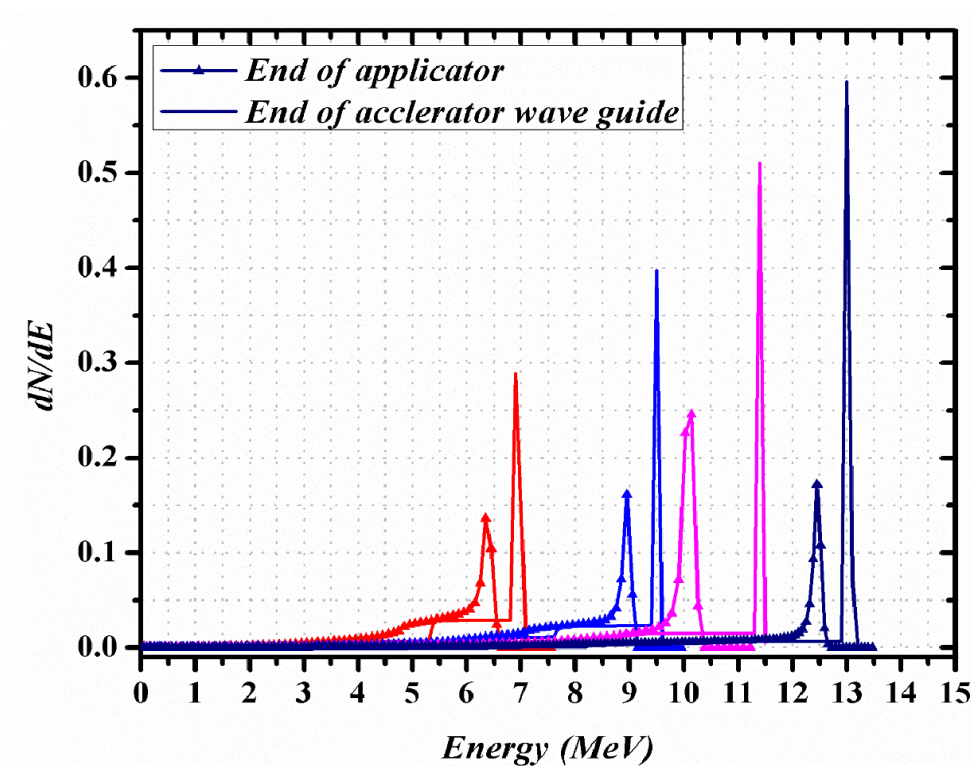


Figure 6: Electron energy spectra at the end of applicator and the end of accelerator wave guide with nominal energies of 6, 8, 10 and 12 MeV and the PMMA applicator of 10 cm diameter.

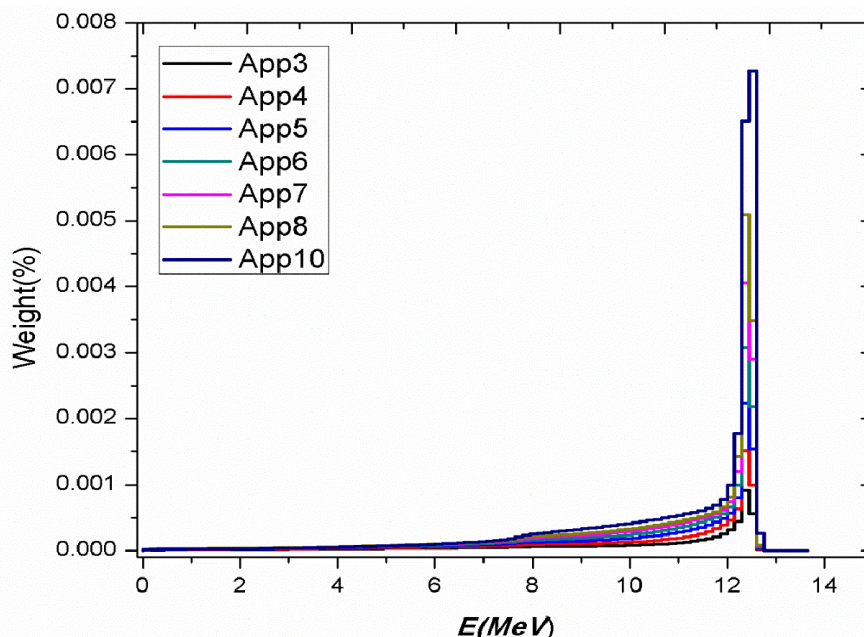


Figure 7: Energy spectrum of 12 MeV electron beam with 3 to 10 cm applicator sizes.

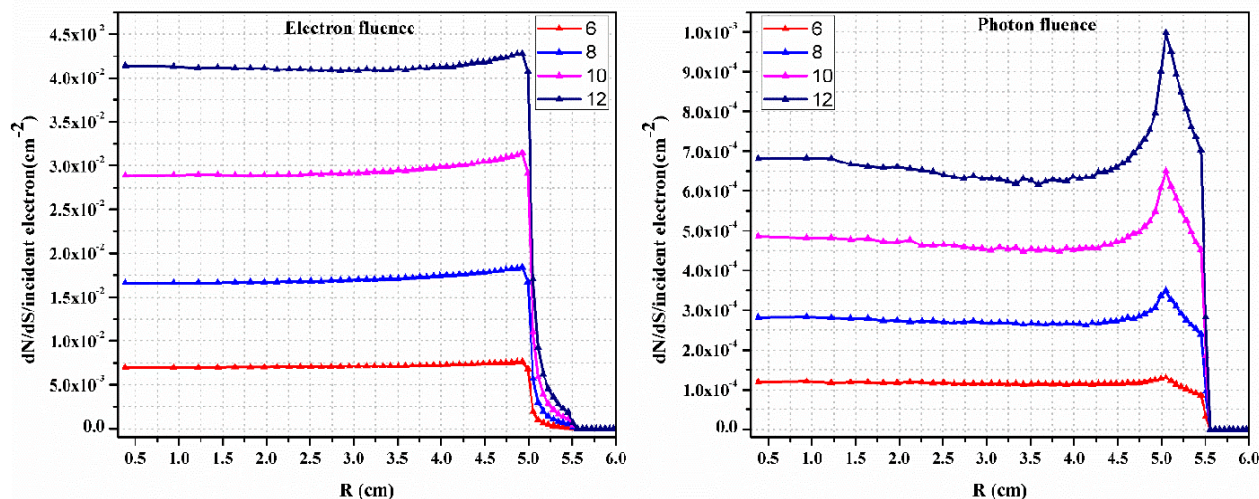


Figure 8: The electron and photon fluence profiles of all nominal energies at the exit of reference applicator.

by changing mentioned parameters [5, 13, 15]. This can be due to the application of cylindrical PMMA applicators in IORT. Increasing these parameters causes divergence of the beam and makes TDPs wide and causes mismatching of these calculated parameters with the measured data. However, application of cylindrical PMMA applicator led to multiple scattering of the electron beams through the

applicator and align the beam to surface of the water phantom.

Figure 6 shows the electron energy spectra at the end of accelerator waveguide and the end of applicator for the beams of 6, 8, 10 and 12 MeV. As it can be seen, there is a decrease in the peak of the spectrum when electrons come from the end of accelerator wave guide to the end of applicator. This is due to mul-

multiple scattering of the electrons through the PMMA applicator. Bjork et al. found about 0.6 MeV difference between conventional (without applicator) and IORT (with applicator) beams for the most probable energies [13]. They mentioned this is mainly due to PMMA scattering with 0.3 cm thickness at the level above the PMMA applicator which was used to increase the surface dose [16]. In addition, they showed that the IORT spectra contain a large number of low-energy electrons in comparison with the conventional beam. The low-energy component of electron beam decreases with increasing the nominal energy of electron beam. Application of this collimator system in dedicated IORT linacs affects the electron energy in phantom surface. As it is shown in Figure 7, the low-energy component of electron beams increases with decreasing the applicator diameter at the end of applicators. These variations led to a decrease of mean and probable energy of degraded electron at the end of applicators. Quantitative results of this analysis are demonstrated in Table 2. Changing the electron beam energy affects the penetration and lateral scattering of electron beams. The effect of changes on the beam energy due to multiple scattering of electron beam can be seen in Figure 7. By decreasing the applicator diameter, the mean energy of electron beam decreased. This leads to rapid fall of PPD curves relative to reference applicator. In addition, by decreasing beam energy, lateral scattering occurred. Furthermore, as it can be seen in the study of Pimpinella and Baghani et al., this change in electron beam energies leads to an increase of output factor by the decrease of applicator size [1, 17].

Radiation protection and photon contamination of electron beams produced by IORT linacs are our major concerns in using these linacs [18, 19]. The main sources of X-ray contamination in medical linacs are the bending magnet, scattering foil and collimation system including collimator jaws [1]. Unlike conventional accelerators, there is no X-ray

adjustable jaw or bending magnet in the LIAC structure. Therefore, the photon contamination remains at lower level, at all energies. The quantitative analysis of our results reveals that there is negligible X-ray contamination for irradiation without applicator as open field by LIAC accelerator. Besides, using applicators and increasing of their size, X-ray contamination will increase. It can be concluded that using PMMA applicator in these linacs leads to, although well below the accepted level, the production of bremsstrahlung. The effect of using PMMA applicator on photon contamination can be seen in Figure 6. Increasing photon fluence at the edge of the fields can be primarily due to the bremsstrahlung production following the striking of electrons to the PMMA. The percentage of X-ray contamination increases by applicator diameter. This is related to the increase of the mean energy of electron beams. These results were in good agreement with the results of Righi et al. [4]. Furthermore, our results on the X-ray contamination are in agreement with the results of Baghani et al. [1].

Conclusion

Application of PMMA collimator may change the characteristic of the electron beam produced by these types of accelerators. Regarding the fact that the surface is considered as a part of treatment target in IORT due to high probability of tumour cells in the vicinity of the gross tumour, it is important to be assured about the adequate dose on the surface. The multiple scattering effect of PMMA applicators and no bending magnet usage in the head of this dedicated accelerator lead to the presence of low component electrons in the produced beam which compensates for the need of sufficient surface dose.

Furthermore, the results of this study showed that special design of LIAC head accompanying by PMMA collimator system produce electron beam with a unique dosimetric characteristic making it a useful tool for intraop-

erative radiotherapy purposes.

Conflict of Interest

None

References

1. Baghani HR, Aghamiri SM, Mahdavi SR, Akbari ME, Mirzaei HR. Comparing the dosimetric characteristics of the electron beam from dedicated intraoperative and conventional radiotherapy accelerators. *J Appl Clin Med Phys*. 2015;**16**:5017. doi: 10.1120/jacmp.v16i2.5017. PubMed PMID: 26103175.
2. Laitano RF, Guerra AS, Pimpinella M, Caporali C, Petrucci A. Charge collection efficiency in ionization chambers exposed to electron beams with high dose per pulse. *Phys Med Biol*. 2006;**51**:6419-36. doi.org/10.1088/0031-9155/51/24/009. PubMed PMID: 17148826.
3. Di Martino F, Giannelli M, Traino AC, Lazzeri M. Ion recombination correction for very high dose-per-pulse high-energy electron beams. *Med Phys*. 2005;**32**:2204-10. doi.org/10.1118/1.1940167. PubMed PMID: 16121574.
4. Righi S, Karaj E, Felici G, Di Martino F. Dosimetric characteristics of electron beams produced by two mobile accelerators, Novac7 and Liac, for intraoperative radiation therapy through Monte Carlo simulation. *J Appl Clin Med Phys*. 2013;**14**:3678. PubMed PMID: 23318376.
5. Iaccarino G, Strigari L, D'Andrea M, Bellesi L, Felici G, Ciccotelli A, et al. Monte Carlo simulation of electron beams generated by a 12 MeV dedicated mobile IORT accelerator. *Phys Med Biol*. 2011;**56**:4579-96. doi.org/10.1088/0031-9155/56/14/022. PubMed PMID: 21725139.
6. Rogers DW, Faddegon BA, Ding GX, Ma CM, We J, Mackie TR. BEAM: a Monte Carlo code to simulate radiotherapy treatment units. *Med Phys*. 1995;**22**:503-24. doi.org/10.1118/1.597552. PubMed PMID: 7643786.
7. Rogers D, Ma C, Walters B, Ding G, Sheikh-Bagheri D, Zhang G. BEAMnrc Users Manual National Research Council of Canada. NRCC Report PIRS-0509 (A) revK. 2002.
8. Bielajew AF, Rogers D. PRESTA: the parameter reduced electron-step transport algorithm for electron Monte Carlo transport. *Nuclear Instruments and Methods in Physics Research Section B: Beam Interactions with Materials and Atoms*. 1986;**18**:165-81. doi.org/10.1016/S0168-583X(86)80027-1.
9. Walters B, Kawrakow I, Rogers D. DOSXYZnrc users manual. NRC Report PIRS. 2005;794.
10. Low DA, Harms WB, Mutic S, Purdy JA. A technique for the quantitative evaluation of dose distributions. *Med Phys*. 1998;**25**:656-61. doi.org/10.1118/1.598248. PubMed PMID: 9608475.
11. Low DA, Dempsey JF. Evaluation of the gamma dose distribution comparison method. *Med Phys*. 2003;**30**:2455-64. doi.org/10.1118/1.1598711. PubMed PMID: 14528967.
12. Ma C, Rogers D. BEAMDP users manual. NRC Report PIRS-0509 (D). 1995.
13. Bjork P, Nilsson P, Knoos T. Dosimetry characteristics of degraded electron beams investigated by Monte Carlo calculations in a setup for intraoperative radiation therapy. *Phys Med Biol*. 2002;**47**:239-56. doi.org/10.1088/0031-9155/47/2/305. PubMed PMID: 11837615.
14. Mihailescu D, Pimpinella M, Guerra A, Laitano R. Comparison of measured and Monte Carlo calculated dose distributions for the NOVAC7® linear accelerator. *Romanian Journal of Physics*. 2006;**51**:729.
15. Bjork P, Knoos T, Nilsson P. Influence of initial electron beam characteristics on monte carlo calculated absorbed dose distributions for linear accelerator electron beams. *Phys Med Biol*. 2002;**47**:4019-41. doi.org/10.1088/0031-9155/47/22/308. PubMed PMID: 12476980.
16. Bjork P, Knoos T, Nilsson P, Larsson K. Design and dosimetry characteristics of a soft-docking system for intraoperative radiation therapy. *Int J Radiat Oncol Biol Phys*. 2000;**47**:527-33. doi.org/10.1016/S0360-3016(00)00456-9. PubMed PMID: 10802382.
17. Pimpinella M, Mihailescu D, Guerra AS, Laitano RF. Dosimetric characteristics of electron beams produced by a mobile accelerator for IORT. *Phys Med Biol*. 2007;**52**:6197-214. doi.org/10.1088/0031-9155/52/20/008. PubMed PMID: 17921580.
18. Beddar AS, Biggs PJ, Chang S, Ezzell GA, Faddegon BA, Hensley FW, et al. Intraoperative radiation therapy using mobile electron linear accelerators: Report of AAPM Radiation Therapy Committee Task Group No. 72. *Medical physics*. 2006;**33**:1476-89. doi.org/10.1118/1.2194447.
19. Robotjazi M, Mahdavi SR, Takavr A, Baghani HR. Application of Gafchromic EBT2 film for intraoperative radiation therapy quality assurance. *Phys Med*. 2015;**31**:314-9. doi.org/10.1016/j.ejmp.2015.01.020. PubMed PMID: 25703011.